ELECTROMAGNETIC TRANSMISSION AND DETECTION AT DEEP DEPTHS

D. B. Starkey
Acceptance Technology Division 8344
Sandia Laboratories Livermore

Introduction

Investigation into the expressions of the field produced by a loop over a conducting half space or in an infinite conducting half space are well documented. Reasonably complex descriptions of the effects of stratification also are reported. However, a model which must contain all of these complexities because of transmission to depths of 15,000 feet and also include the pertibation of the field by a verticle cylindrical steel casing loses its facility in the field or for quick, accurate approximation to field magnitudes and phase.

This paper describes the results of two field tests to determine the attenuation and phase versus depth and frequency of an electromagnetic wave (induction field). A simple two-layer model is postulated to predict the magnitude and phase of the induced field which does not require sophisticated computing tools. Correlation of the model with experimental results show agreement of most amplitude measurements to within 3 db and most phase measurements to within five degrees. The tests were conducted in a 7400 foot deep well in Nevada and an 11,000 foot deep well in Wyoming which had conductivities ranging from .0025 mhos/m to .25 mhos/m. The surface transmitting dipole had an area of $\sim 10^6$ feet squared and constant frequency signals of 1.5 Hz to 20 Hz were transmitted through the earth utilizing less than 65 watts of power.

Model Description

The magnetic field intensity components generated by a magnetic dipole immersed in an infinite homogeneous medium can be expressed in spherical coordinates as:

$$H_r = \frac{NI\ (\pi a^2)}{4\pi r^3}\ [1 + \gamma r]\ [e^{-\gamma r}]\ 2\cos\theta \tag{1}$$

$$H_\theta = \frac{NI\ (\pi a^2)}{4\pi r^3}\ [1 + \gamma + \gamma^2 r^2]\ [e^{-\gamma r}]\ \sin\theta \tag{2}$$

$$r = (Z^2 + a^2)^{1/2}$$
Z = verticle depth between coaxial loops

where N, I, and (πa^2) are the transmitting antenna turns, current, and effective area, respectively, and r is the range from the loops circumference to the measurement point. The case of interest for these experiments, however, is the special case of coaxial dipoles, i.e., $\theta = 180°$. For this case $H_\theta = 0$ and H_r reduces to:

$$H_r = \frac{NI\ (\pi a^2)}{2\pi r^3}\ [1 + \gamma r]\ [e^{-\gamma r}] \tag{3}$$

It is apparent from the expression for r that dipoles of finite dimensions are being considered. For these tests the radius was either 600 or 1200 feet and the effect of the loop's radius had to be considered.

The complex propagation constant, γ, is expressed in terms of angular frequency, $\omega = 2\pi f$ and the medium properties conductivity, σ, permeability, μ, and permittivity, ε. For conducting media, displacement current effects are generally negligible and for the condition $\sigma >> \omega\varepsilon$

$$\gamma \simeq (1 + j) \left(\frac{\omega\mu\sigma}{2}\right)^{1/2}$$

where the skin depth δ is the inverse of real part of γ or

$$\delta = (2/\omega\mu\sigma)^{1/2}$$

Although in the actual experiments, there is a half space of air above the ground, the increased complexity of the model including this half space was not considered practical. This appears to be justified in examining the results of the two field experiments.

Media Discontinuity

Because of the depths involved in the experiments, stratification of the media is obvious from the available lithologies. Although consideration was given to characterize the media from a single lumped homogeneous, isotropic region with an average conductivity to n homogeneous, isotropic regions as dictated by the lithology, the end result was to use a two-layer model. The single homogeneous layer appeared impractical when one studied the DC resistivity logs of the experimental wells. Although the resistivity varied over quite a dynamic range, there seemed to be two or three "average" values which fit only a particular depth increment. The n layer model was discarded also because it did not fit the resistivity logs. In addition, because of the wavelengths involved, many thin layers of different conductivity can be ignored because only small phase delays are encountered in a layer, resulting approximately in cancellation of the two reflections.

The resulting two-layer solution is shown below:

$$H_r(Y + X) = H_r(Y) \left(\frac{Y}{Y + X}\right)^3 (1 + \gamma_2 Z_2) \left(e^{-\gamma_2 Z_2}\right) \qquad (4)$$

where Y = radius at the interface $(Z_1^2 + a^2)^{1/2}$

X = radius below the interface $(Z^2 + a^2)^{1/2}$

$H_r(Y)$ = magnetic field intensity at interface from Equation 3

γ_2 = propagation constant for the second layer

Z_1 = verticle depth from transmitting loop to interface

Z_2 = verticle depth from interface to receiving loop

Well Casing Attenuation

Assuming that the resultant field from the above calculations is that which is present at any depth, the attenuation of the magnetic field intensity by the well casing is calculated by the following relationship described by Shenfeld for infinite long cylinders whose radius is much greater than the cylinder thickness:

$$\frac{\overline{H}_o}{\overline{H}_i} = \cosh(\overline{\gamma}d) + \frac{\mu_o}{2\mu}\gamma\,\delta\,r\,\sinh(\overline{\gamma}d)$$

$\overline{H}_o$ = magnetic field intensity outside the cylinder

$\overline{H}_i$ = magnetic field intensity inside the cylinder

$\overline{\gamma}$ = propagation constant for the wall material

δ = skin depth in the wall material

μ = wall material permeability (200 μ_o)

r = cylinder radius

d = cylinder wall thickness

The above expression is said to be valid for the following cases:

1. High or low frequencies (converges to the skin depth solution at high frequencies)
2. Magnetic or non-magnetic wall material
3. Orientation of H_o is unimportant

Although this expression diverges somewhat from the concept of developing a simple model, it is required at the frequencies of interest (below 20 Hz). Figure 1 is a plot of the attenuation from Shenfeld's relationship and plane wave attenuation from .1 to 10 Hz for a typical casing. It can be seen that even at 10 Hz the plane wave attenuation is ∿ 6 db pessimistic relative to Shenfeld's formulation. Multiple casings encountered in some of the testing are handled as a single cylinder whose thickness is equal to the sum of all the casings' thickness.

Receiving Antenna

The receiving antenna is a ferrite loop stick in construction. Assuming that the core "captures" all of flux within the casing and that this flux is uniformly distributed across the internal cross section, the open circuit voltage from the antenna is described as follows:

$$|V| = \omega\mu_o A_{eff} |\overline{H}_i|$$

$|\overline{H}_i|$ = magnitude of Shenfeld's internal field intensity

A_{eff} = effective area of the receiving antenna

ω = angular frequency

μ_o = free space permeability

Since $\overline{H}_i$ for a given depth and media decreases with frequency and the voltage output has frequency as a multiplier, an optimum frequency is expected. The model (using the Wyoming data below) shows an optimum at ∿ 2 Hz at 6000 feet and ∿ 1 Hz at 12,000 feet.

Test Apparatus

Figure 2 is a block diagram of the test apparatus used to gather the data for both test series. A square wave oscillator is set at the desired frequency. The phase of this signal relative to that which is the reference for a coherent detector can be selected at either 0 or 45 degrees. The square wave is then filtered and its gain controlled to drive the output of an audio amplifier. The transmitting loop has a .05 ohm resistor in series such that the current in the loop can be determined and the phase shift of the amplifier removed from the phase measurements. The signal received downhole is then amplified by either 130 or 160 db and used as an input to a 1 KHz VCO. This signal is brought uphole on a cable, discriminated, filtered, and fed to the coherent detector. The detector outputs then give a real time indication of the received signal characteristics as follows:

$$V_{\text{received RMS}} = \sqrt{I^2 + Q^2} \Big/ \text{Gain}$$

$$\phi_{\text{path}} = \tan^{-1} Q/I - (\text{receiver and transmitter phase})$$

The 3 db bandwidth of the amplifying system was from $\sim$ .9 Hz to 30 Hz. The coherent detector's bandwidth was generally left at .025 Hz.

Nevada Test Site and Model Parameters

Figure 3 is a graphic view of the NTS test configuration. A double casing extended to a depth of 940 feet. From this depth to 7410 feet a single casing was present. The model parameters used were:

Interface Depth: Z_1 = 1500 feet

Layer One: σ = .0025 mhos/m

Layer Two: σ = .01 mhos/m

Two transmitting loops were used, each with an area of $\sim 10^6$ feet^2. One was offset approximately 1200 feet from the well center. The transmitted power (I^2R losses) was varied from 4 to 13 watts with signal-to-noise ratios at 5 Hz varying from 35 to 12 db at 1000 and 7410 feet respectively. The offset antenna was used among other techniques to give assurance that the signal was not propagated down the cable or well casing--since the phase would be different for this case versus through the earth, particularly at the shallow depths. Figures 4, 5, and 6 show the relative strengths of the measured fields as compared to the model predictions.

Wyoming Tests

Figure 7 is a graphic view of the Wyoming test configuration. A triple casing extended to 437 feet. From 437 feet to 8255 feet a double casing existed and below 8255 to 11,000 feet only a single casing was present. The model parameters used were:

Interface Depth: 8100 feet

Layer One: σ = .05 mhos/m

Layer Two: σ = .25 mhos/m

One transmitting loop was used with an area of 4×10^6 feet^2. The transmitter power was varied from 4 to 65 watts with signal-to-noise ratios at 5 Hz varying from 20 db to 2 db at 3500 feet and 11,000 feet respectively. Figures 8, 9, and 10 show the relative strengths of the measured fields.

Discussion of Results

The correlation between calculated and experimental values indicates that the model is extremely accurate. Although the phase plots have been omitted because of space limitations, the two-layer model is also capable of high accuracy in this prediction at all depths also. Only at the shallow depths is the phase prediction high by approximately five degrees. The use of the infinite homogeneous model appears to balance any effects in the field caused by the steel casing.

The amplitude plots show a discontinuity at the location of a change in the number of casings. This fact, plus the use of the offset antenna at NTS, show that the signal is propagating in the medium and not down the casing. Additional calculations yielded a maximum attenuation rate of only .9 db/1000 feet presuming the signals was coupled down the armored cable used to lower the receiving package. Since the actual attenuation rates were much greater, this was also eliminated as a possible coupling link.

Acknowledgements

This work was supported by the United States Atomic Energy Commission Division of Peaceful Nuclear Explosives, Contract Number AT-(29-1)-789.

The author would also like to thank El Paso Natural Gas Company for providing the test well and their capable assistance in the conduction of the Wyoming experiment.

References

1. S. Shenfeld, "Shielding of Cylindrical Tubes", IEEE Transactions on Electromagnetic Compatibility, Volume EMC-10, No. 1, March 1968

2. James R. Wait, "Electromagnetic Fields of Sources in Lossy Media", Antenna Theory: Part II, McGraw-Hill Book Company, 1969

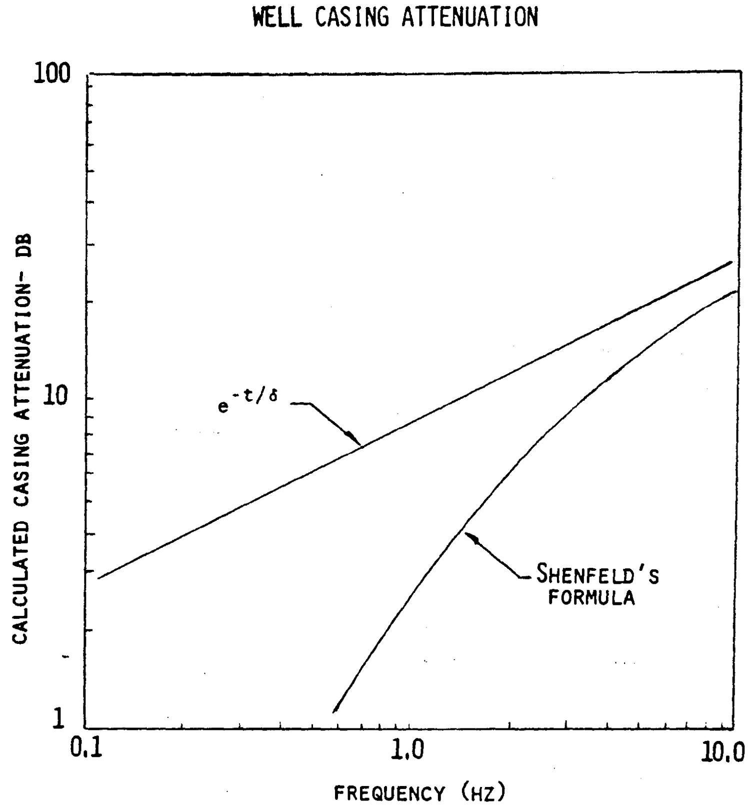

Figure 1

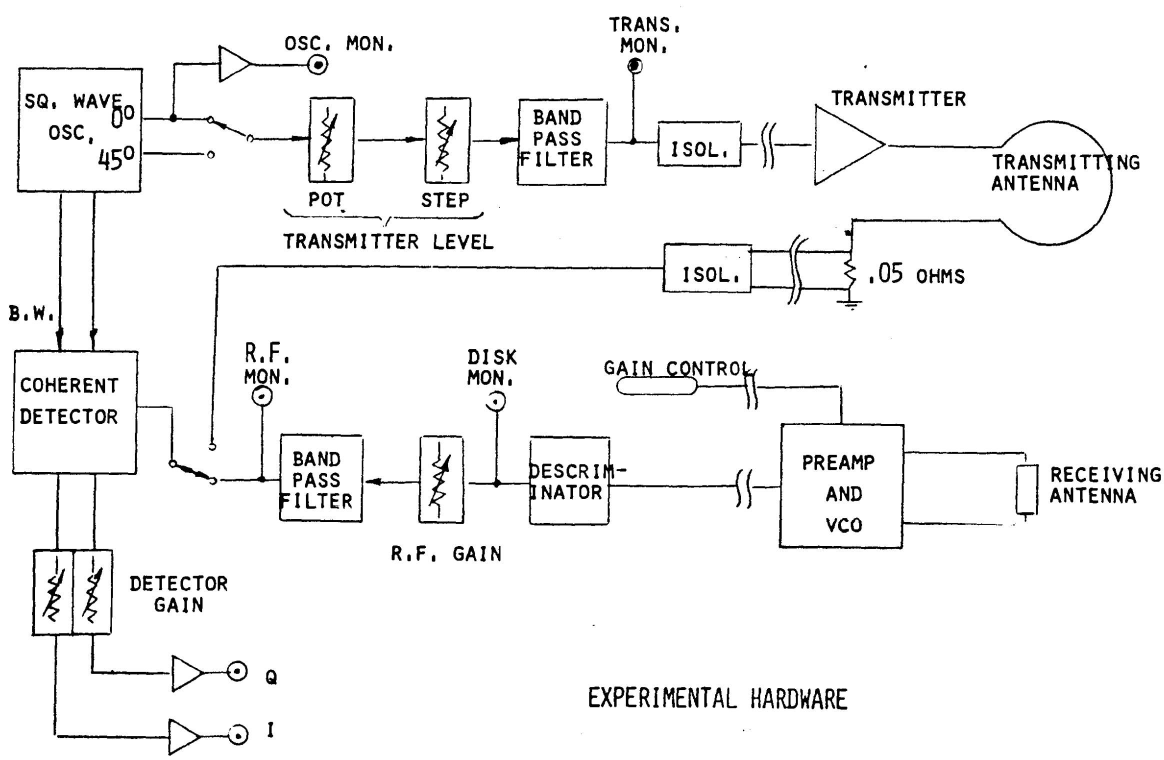

Figure 2

NTS TESTS - AREA 20

PAHUTE #1

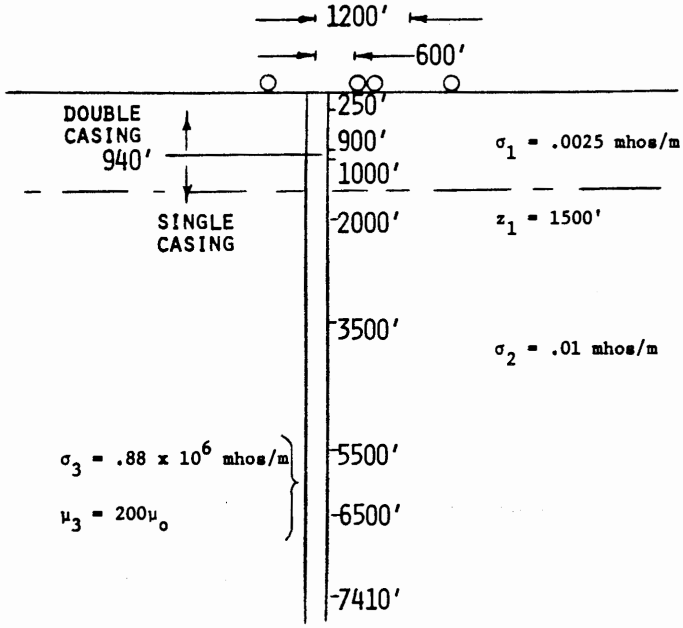

Figure 3

WYOMING TESTS

EP #5

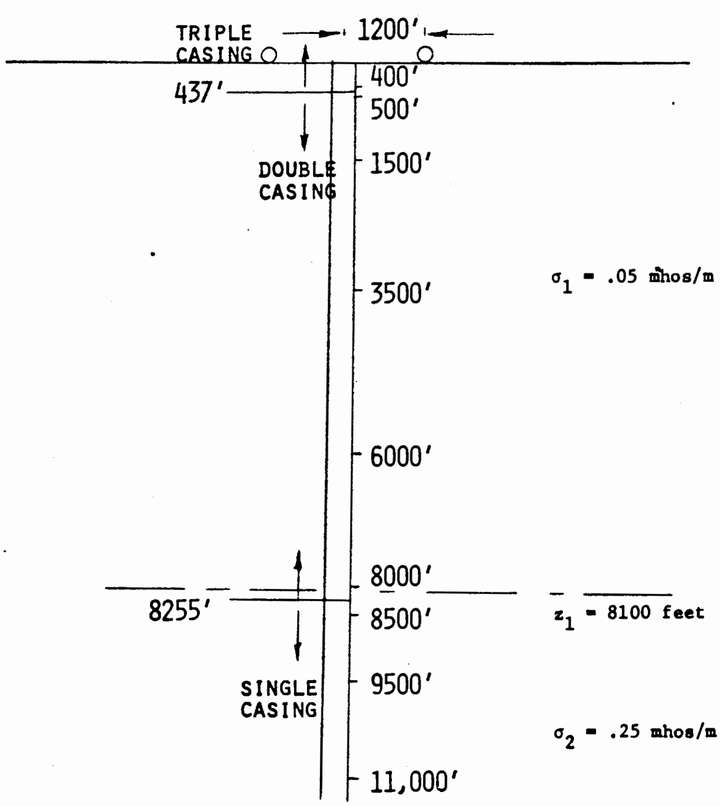

Figure 7

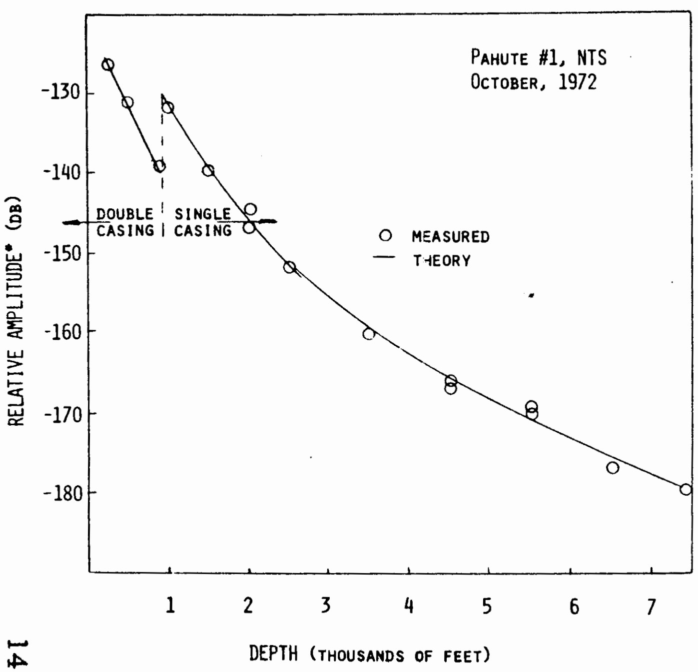

*Signals relative to 1 volt RMS at the receiving antenna for 1 amp RMS in the transmitting loop.

Measured attenuation rate: ~4.4 dB/1000 feet (last 3500 feet)

5 Hz SIGNAL ATTENUATION

Figure 4

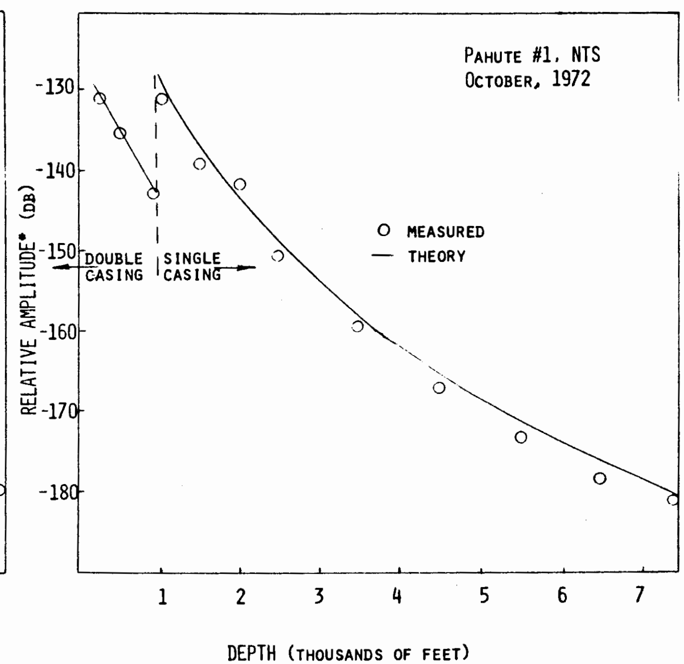

*Signals relative to 1 volt RMS at the receiving antenna for 1 amp RMS in the transmitting loop.

Measured attenuation rate: ~4.8 dB/1000 feet (last 3500 feet)

10 Hz SIGNAL ATTENUATION

Figure 5

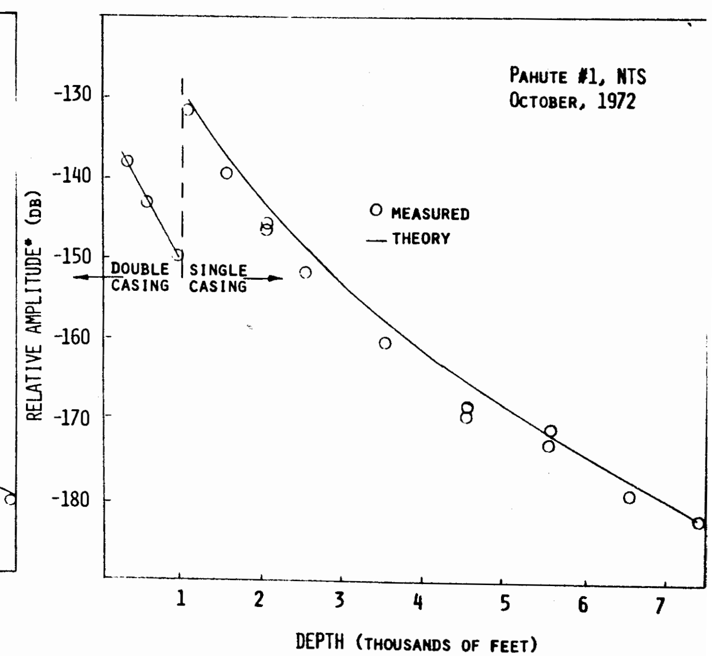

*Signals relative to 1 volt RMS at the receiving antenna for 1 amp RMS in the transmitting loop.

Measured attenuation rate: ~5.1 dB/1000 feet (last 3500 feet)

20 Hz SIGNAL ATTENUATION

Figure 6

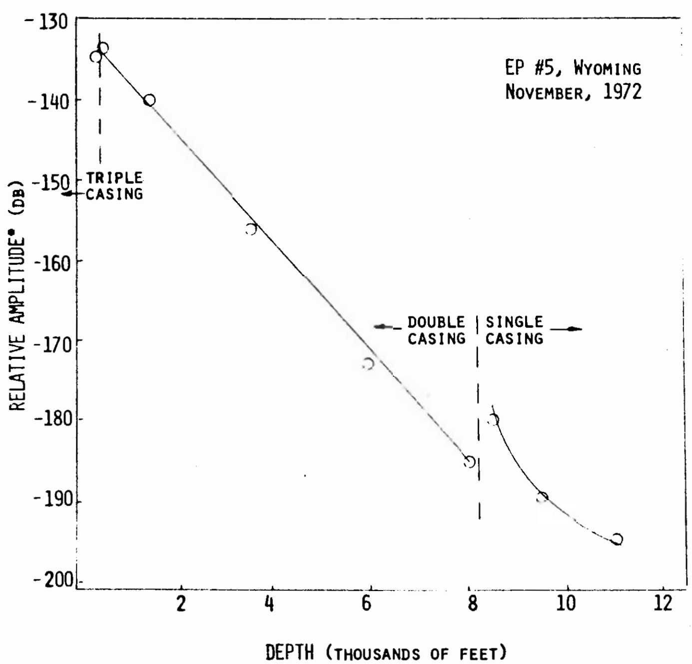

*Signals relative to 1 volt RMS at the receiving antenna for 1 amp RMS in the transmitting loop.

Measured attenuation rate: ~7.1 dB/1000 feet (double casing)

5 Hz Signal Attenuation

Figure 8

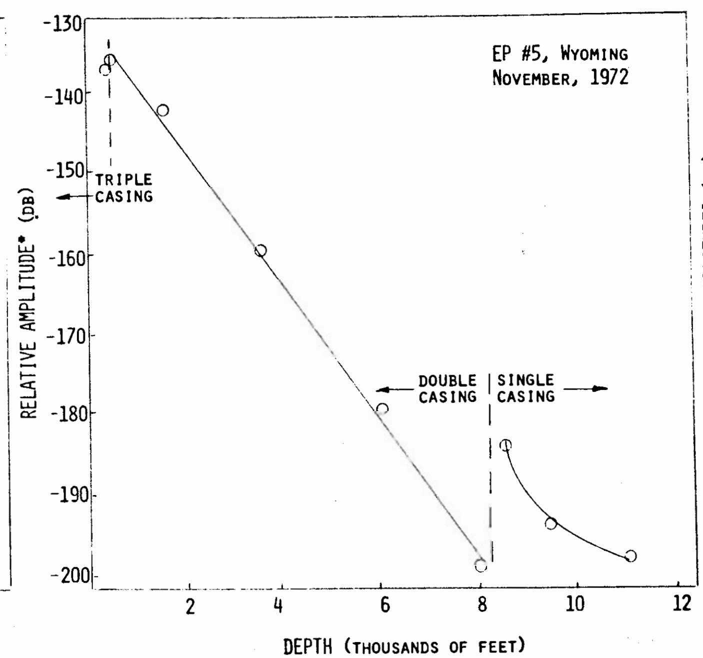

*Signals relative to 1 volt RMS at the receiving antenna for 1 amp RMS in the transmitting loop.

Measured attenuation rate: 8.4 dB/1000 feet (double casing)

10 Hz Signal Attenuation

Figure 9

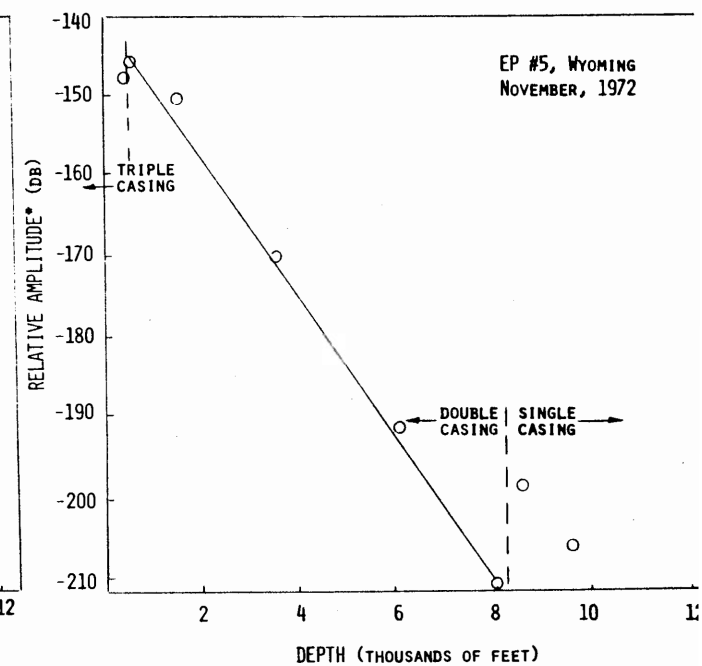

*Signals relative to 1 volt RMS at the receiving antenna for 1 amp RMS in the transmitting loop.

Measured attenuation rate: ~8.7 dB/1000 feet (double casing)

20 Hz Signal Attenuation

Figure 10